

# Muonium-antimuonium conversion in models with heavy neutrinos

Gorazd Cvetič\* and Claudio O. Dib†

*Dept. of Physics, Universidad Técnica Federico Santa María, Valparaíso, Chile*

C. S. Kim‡

*Department of Physics, Yonsei University, Seoul 120-749, Korea*

J. D. Kim§

*Department of Physics, Seoul National University, Seoul 151-742, Korea*

(Dated: 11 April 2005)

We study muonium-antimuonium conversion and  $\mu^+e^- \rightarrow \mu^-e^+$  scattering within two different lepton-flavor-violating models with heavy neutrinos: model I is a typical seesaw that violates lepton number as well as flavor; model II has a neutrino mass texture where lepton number is conserved. We look for the largest possible amplitudes of these processes that are consistent with current bounds. We find that model I has very limited chance of providing an observable signal, except if a finely tuned condition in parameter space occurs. Model II, on the other hand, requires no fine tuning and could cause larger effects. However, the maximum amplitude provided by this model is still two orders of magnitude below the sensitivity of current experiments: one predicts an effective coupling  $G_{M\bar{M}}$  up to  $10^{-4}G_F$  for heavy neutrino masses near 10 TeV. We have also clarified some discrepancies in previous literature on this subject.

## I. INTRODUCTION

Muonium is a hydrogenlike system of an electron ( $e^-$ ) bound to a positive muon ( $\mu^+$ ) and antimuonium is the bound state of the respective antiparticles ( $\mu^-e^+$ ). It is formed as muons stop inside matter, although the fraction of stopped muons that actually form muonium depends very much on the material itself. Since it has no hadronic constituents, muonium is an ideal place to test electroweak interactions. In particular, since conversion of muonium into antimuonium is completely forbidden within the standard model (SM) because it violates lepton flavor, its observation will be a clear signal of physics beyond the SM. This phenomenon was first suggested almost 50 years ago [1] and since then several studies [2, 3] and experimental searches [4] have been done. Many extensions of the SM could cause muonium to antimuonium conversion [5] (left-right symmetric gauge models, extra neutrinos, extra higgses, SUSY, bileptonic gauge bosons, etc).

Here we want to study the possibility that heavy Majorana neutrinos in models of seesaw type could cause an observable signal of muonium-antimuonium conversion. In previous works we have studied the prospects for these models to generate tau decays that violate lepton flavor [6]. The main feature of these models is that they only extend the standard model by the existence of extra neutral leptons. The most natural scenario is then that lepton families will mix (thus destroying lepton flavor conservation) and that neutrinos will acquire masses. In order to insure that the standard neutrinos remain light, the texture of the neutrino mass matrix should favor a seesaw type of mechanism. In these models, muonium to antimuonium conversion appears at one loop level in the perturbative expansion (box diagrams –see Figs. 1 and 2) and it is thus a very small effect.

A simple estimate of this conversion probability within the models in question shows that it is too small to be observed in foreseeable experiments [7]. Another work along these lines [8], making a rough estimate shows that present experimental bounds set a lower bound on large Majorana masses at around  $10^1$  TeV. However, we find that the validity of the calculation (perturbation theory to one loop) breaks down for masses above that same scale. Therefore one can make clear predictions for masses up to that scale only. We analyze the process in more detail within the one-loop approximation, performing a comprehensive search for the bounds in the currently allowed parameter space. We confirm the conclusion that seesaw models give a conversion probability that is still too small to be at the reach of experiments to date. We also find that typical seesaw models of heavy neutrinos are in most cases totally out

---

\*Electronic address: gorazd.cvetic@usm.cl

†Electronic address: claudio.dib@usm.cl

‡Electronic address: cskim@yonsei.ac.kr

§Electronic address: jade@phya.snu.ac.kr

of reach of any foreseeable experiment, except in very special, fine-tuned regions of the parameter space. In contrast, models with heavy neutrinos that conserve lepton number give conversion probabilities closer to present experimental sensitivities for natural values of parameters.

In section II we give the generalities of muonium-antimuonium conversion; in section III we calculate the process within the models in question and do a comprehensive search of the presently allowed parameter space, looking for the maximal possible conversion probabilities. In section IV we give brief account of the unbound collision  $\mu^+e^- \rightarrow \mu^-e^+$  and its prospects. In section V we state our conclusions. Details of the seesaw models and loop calculations are included as appendices.

## II. MUONIUM TO ANTIMUONIUM CONVERSION

Muonium  $|M\rangle$  is a nonrelativistic Coulombic bound state of  $\mu^+$  and  $e^-$ , and antimuonium  $|\bar{M}\rangle$  a similar bound state of  $\mu^-$  and  $e^+$ . The nontrivial mixing between  $|M\rangle$  and  $|\bar{M}\rangle$  comes in our context from the non-vanishing LFV transition amplitude for  $e^-\mu^+ \rightarrow e^+\mu^-$ . In a model with heavy neutrinos, this amplitude appears at one loop (box diagrams) in the electroweak interaction extended with extra (heavy) neutrinos. This transition is usually expressed in terms of a local effective Hamiltonian density with an effective coupling  $G_{M\bar{M}}$ :

$$\mathcal{H}_{\text{eff}}(x) = \frac{G_{M\bar{M}}}{\sqrt{2}} [\bar{\mu}(x)\gamma^\alpha(1-\gamma_5)e(x)] [\bar{e}(x)\gamma_\alpha(1-\gamma_5)\mu(x)] . \quad (1)$$

Due to this interaction,  $|M\rangle$  and  $|\bar{M}\rangle$  are not mass eigenstates. In this basis, the mass matrix has non-diagonal components:

$$m_{M\bar{M}} = \langle M | \int d^3x \mathcal{H}(\mathbf{x}) | \bar{M} \rangle, \quad (2)$$

where the (non-relativistic) bound states are chosen with unit norm in a volume  $V$ , namely  $\langle M(\mathbf{P}) | M(\mathbf{P}') \rangle = (2\pi)^3 \delta^3(\mathbf{P} - \mathbf{P}')/V$ . If we express the bound state in terms of its constituents with a momentum distribution  $f(p)$ :

$$|M(0)\rangle = \int \frac{d^3p}{(2\pi)^3} f(p) a_p^{(e)\dagger} b_{-p}^{(\mu)\dagger} |0\rangle, \quad (3)$$

and neglect the momentum dependence in the spinors, the mass mixing element is:

$$m_{M\bar{M}} = 16 \frac{G_{M\bar{M}}}{\sqrt{2}} \left| \int \frac{d^3p}{(2\pi)^3} f(p) \right|^2 \bar{u}_{(\mu)L} \gamma^\alpha u_{(e)L} \bar{v}_{(\mu)L} \gamma_\alpha v_{(e)L} \quad (4)$$

Since angular momentum is conserved, the only non vanishing elements are those where the spin of the initial and final bound state are the same. For both the singlet or each of the triplet components, the spinor product has the same value  $2m_\mu m_e$  [9]. Additionally, the integral of  $f(p)$  is the spatial wavefunction at zero distance,  $|\int d^3p/(2\pi)^3 f(p)|^2 = |\Psi(0)|^2/(2m_\mu 2m_e)$ . The mass mixing element [10] thus reduces to

$$m_{M\bar{M}} = 16 \frac{G_{M\bar{M}}}{\sqrt{2}} \frac{|\Psi(0)|^2}{2} = 16 \frac{G_{M\bar{M}}}{\sqrt{2}} \frac{(\mu\alpha)^3}{2\pi} \quad (5)$$

where  $\mu \approx m_e$  is the muonium reduced mass and  $\alpha$  the fine structure constant. In vacuum, the diagonal mass terms are equal,  $m_{MM} = m_{\bar{M}\bar{M}}$ . The mass eigenstates are then the simple combinations  $|M_1\rangle = (|M\rangle + |\bar{M}\rangle)/\sqrt{2}$  and  $|M_2\rangle = (|M\rangle - |\bar{M}\rangle)/\sqrt{2}$  and the mass eigenvalues differ in  $\Delta m \equiv m_1 - m_2 = 2 m_{M\bar{M}}$ . This is the typical case of a quantum system of two states that oscillate into each other under time evolution, like the  $K^0 - \bar{K}^0$  system in hadrons. However, unlike the latter, in practical terms muonia do not have time to show an oscillation, because their oscillation time is much longer than their decay time. So one can only hope to observe the mixing phenomenon by measuring the probability that a state that starts as a Muonium ( $\mu^+e^-$ ) decays as an Antimuonium (decay into a high energy electron and low energy positron). So, the state that starts as  $|M\rangle$  at  $t = 0$  (call it  $|M(t)\rangle$ ) evolves as:

$$|M(t)\rangle = |M_1\rangle \langle M_1 | M \rangle e^{-i m_1 t} + |M_2\rangle \langle M_2 | M \rangle e^{-i m_2 t} \quad (6)$$

and will decay as a  $\bar{M}$  with a total probability:

$$P(M \rightarrow \bar{M}) = \int_0^\infty \frac{dt}{\tau} e^{-t/\tau} |\langle \bar{M} | M(t) \rangle|^2 = \frac{(\Delta m \tau)^2}{2(1 + (\Delta m \tau)^2)} \approx \frac{1}{2} (\Delta m \tau)^2 \quad (7)$$

$P(M \rightarrow \bar{M})$	$G_{M\bar{M}}/G_F$	Experiment
$< 2.1 \times 10^{-6}$	$< 0.29$	Huber et al. (1990)
$< 6.5 \times 10^{-7}$	$< 0.16$	Matthias et al. (1991)
$< 8.0 \times 10^{-9}$	$< 1.8 \times 10^{-2}$	Abela et al. (1996)
$< 8.3 \times 10^{-11}$	$< 3 \times 10^{-3}$	Willmann et al. (1999)

TABLE I: Experimental results (see Ref. [4]) for the conversion probability and the deduced upper bound for the coupling  $G_{M\bar{M}}$  (this bound on the last row is weaker than what Eq. (8) gives, because of magnetic field suppression).

where  $\tau$  is the muon lifetime. Eq. (7) does not take into account the effect of static electromagnetic fields in materials, which break the degeneracy  $m_{MM} = m_{\bar{M}\bar{M}}$  and cause an extra suppression on the probability[2], an important effect in some experiments. In any case, we see from Eq. (7) that the conversion probability is in general very small and proportional to  $|G_{M\bar{M}}|^2$ :

$$P(M \rightarrow \bar{M}) = \frac{64 G_F^2 \alpha^6 m_e^6 \tau^2}{\pi^2} \left( \frac{G_{M\bar{M}}}{G_F} \right)^2 = 2.64 \times 10^{-5} \left( \frac{G_{M\bar{M}}}{G_F} \right)^2. \quad (8)$$

The experiments so far have gradually been improving on an upper bound for  $P(M \rightarrow \bar{M})$  and thus for  $G_{M\bar{M}}$  (See Table 1), but no positive signal of this lepton flavor violating process has ever been observed, which is consistent with the null prediction of the standard model. All new physics in this process enters in the parameter  $G_{M\bar{M}}$ . We will now examine the prospects for  $G_{M\bar{M}}$  in extensions of the standard model with extra heavy neutrinos originating in seesaw mechanisms.

### III. PREDICTION OF THE SEESAW MODELS

We want to explore the prediction of lepton flavor violating seesaw models for muonium-antimuonium conversion. The details of the models are given in Appendix A. The main features of these models are that (i) they contain heavy neutrinos, (ii) in their mass basis, the heavy neutrinos couple to charged leptons of different generations under weak interactions (just like the Cabbibo-Kobayashi-Maskawa prescription in the quark sector), thus inducing flavor changing processes (iii) in general the neutrino masses are of Majorana type.

The mixing matrix  $B_{li}$ , which is defined in Appendix A, is the coefficient of the left-handed current that connects a charged lepton of flavor  $l = e, \mu, \dots$  with a neutrino of flavor  $i = 1, 2, \dots$ . In a model with  $N_L$  charged leptons, the first  $N_L$  neutrinos are light (standard) and the rest are heavy. Here we will only consider  $N_L = 2$  to make the estimates. Of course, general lepton flavor mixing would induce many kinds of processes that are not observed in the real world. The non-observation of those processes impose severe bounds on the values of  $B_{li}$ . Here we use the results of the analysis of Ref. ([11]), which establish bounds on combinations of mixing elements characterized by  $(s_L^{\nu_l})^2 \equiv \sum_{i=h} |B_{li}|^2$ , where  $h$  indicates heavy neutrinos, singlets under  $SU(2)_L$ :

$$(s_L^{\nu_e})^2 < 0.005, \quad (s_L^{\nu_\mu})^2 < 0.002, \quad (s_L^{\nu_\tau})^2 < 0.010. \quad (9)$$

As we said, in these models, muonium-antimuonium conversion is induced by the process  $\mu^+ e^- \rightarrow \mu^- e^+$  at one-loop via box diagrams (see Figs. 1 and 2), where the neutrinos appear as internal quanta. The effective coupling  $G_{M\bar{M}}$  is a function of the internal neutrino masses  $m_i$  and mixing parameters  $B_{li}$  that arises from the integrals of the box diagrams:

$$G_{M\bar{M}}/G_F = \frac{\alpha_W}{32\pi} \sum_{i,j=\text{all } \nu's} \left[ 2B_{ei}^* B_{ej}^* B_{\mu i} B_{\mu j} F_{\text{Box}}(x_i, x_j) - (B_{ei}^*)^2 (B_{\mu j})^2 \lambda_i^* \lambda_j G_{\text{Box}}(x_i, x_j) \right], \quad (10)$$

where  $\alpha_W = g^2/4\pi$  is the weak  $SU(2)_L$  fine structure constant,  $x_i = m_i^2/M_W^2$  are the squares of neutrino masses inside the loop in units of the  $W$  boson mass,  $\lambda_i$  are ‘‘creation phases’’ that appear in Majorana fields [14], and  $F_{\text{Box}}(x_i, x_j)$  and  $G_{\text{Box}}(x_i, x_j)$  are the loop functions that appear integrating the ‘‘Dirac boxes’’ of Fig. 1 and the ‘‘Majorana boxes’’ of Fig. 2, respectively (external masses and momenta inside the integrals are neglected as compared to loop momenta). These functions, symmetric under the interchange  $x_i \leftrightarrow x_j$ , are:

$$F_{\text{Box}}(x_i, x_j) = \frac{1}{x_i - x_j} \left\{ \left( 1 + \frac{x_i x_j}{4} \right) \left( \frac{1}{1 - x_i} + \frac{x_i^2}{(1 - x_i)^2} \ln x_i \right) - 2x_i x_j \left( \frac{1}{1 - x_i} + \frac{x_i}{(1 - x_i)^2} \ln x_i \right) \right. \\ \left. - (i \rightarrow j) \right\} \quad (11)$$

$$G_{\text{Box}}(x_i, x_j) = -\frac{\sqrt{x_i x_j}}{x_i - x_j} \left\{ (4 + x_i x_j) \left( \frac{1}{1 - x_i} + \frac{x_i}{(1 - x_i)^2} \ln x_i \right) - 2 \left( \frac{1}{1 - x_i} + \frac{x_i^2}{(1 - x_i)^2} \ln x_i \right) - (i \rightarrow j) \right\} \quad (12)$$

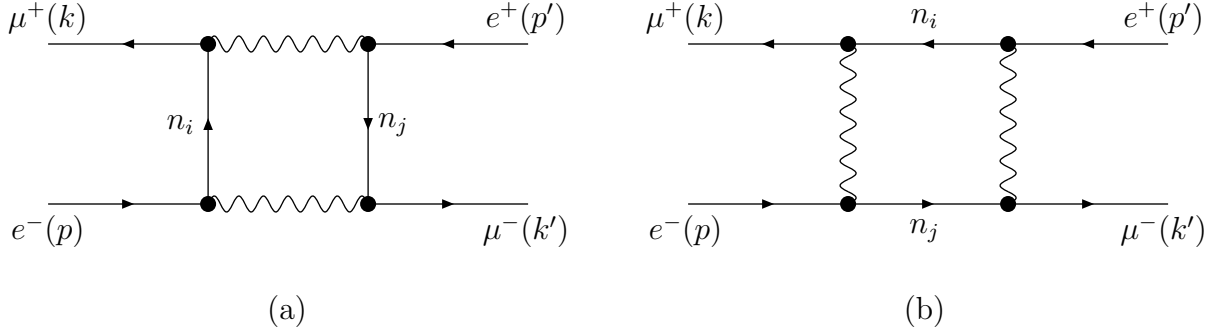


FIG. 1: “Dirac boxes”: box diagrams for generic (Dirac or Majorana) neutrinos (each wavy line is either a  $W$  or a charged Goldstone boson if we work in the Feynman gauge).

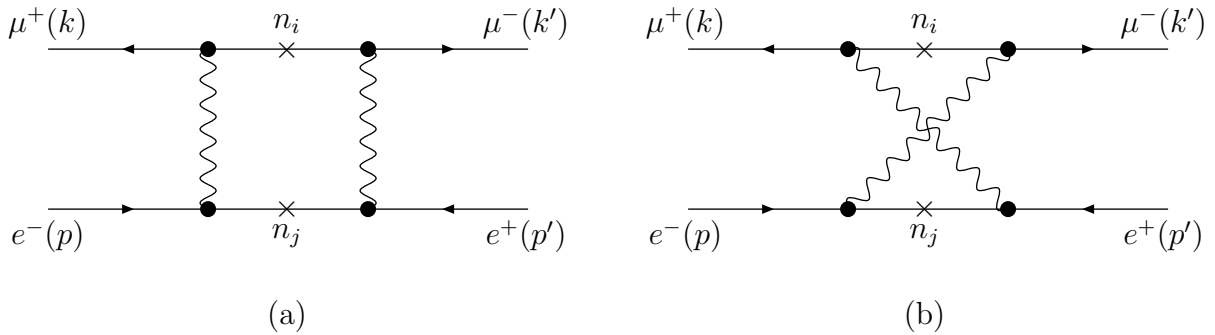


FIG. 2: “Majorana boxes”: box diagrams for Majorana neutrinos only (each wavy line is either a  $W$  or a charged Goldstone boson).

We should point out that we have a discrepancy in the global sign in front of  $G_{\text{Box}}$  in Eq. (10) compared to Ref. [12]. It is important to remark that this global sign can not be changed by simple redefinition of fermion phases. For example, one can redefine the phases of the Majorana fields and choose  $\lambda_i = +1$  for all  $i$ , or equivalently one can absorb those phases in the mixing matrix  $B_{ij}$ , but it is impossible to choose the phases so that  $\lambda_i^* \lambda_j = -1$  for all  $i, j$ . It is also important to notice a discrepancy with Ref. ([8]), where the authors claim that the contribution from the two diagrams of Fig. 2 with Majorana neutrinos (*i.e.* the  $G_{\text{Box}}$  term) cancel because of Fermi statistics. Actually, when one carries through the calculation, the minus sign from Fermi statistics is compensated by the inner structure of the diagrams and at the end both diagrams are equal and they add! Since  $G_{\text{Box}}$  dominates over  $F_{\text{Box}}$  for large neutrino masses, this could be an important issue in the estimates. To clarify these matters, we include the derivation of Eq. (10) in Appendix B.

Using the unitarity of the mixing matrix, Eq. (10) can be rewritten as a double sum over heavy neutrino flavors

only

$$G_{M\bar{M}}/G_F = \frac{\alpha_W}{32\pi} \sum_{I,J=N_L+1}^{N_L+N_H} \left\{ 2B_{eI}^* B_{eJ}^* B_{\mu I} B_{\mu J} [F_{\text{Box}}(x_I, x_J) - 2F_{\text{Box}}(x_I, 0) + F_{\text{Box}}(0, 0)] - (B_{eI}^*)^2 (B_{\mu J})^2 \lambda_I^* \lambda_J G_{\text{Box}}(x_I, x_J) \right\}, \quad (13)$$

where light neutrino masses are neglected.

Table I shows that in order for muonium to antimuonium conversion to be observable in at least the most sensitive experiment to date, the coupling  $G_{M\bar{M}}/G_F$  should be at least  $\mathcal{O}(10^{-3})$ . A rough estimate for the largest value expected for  $G_{M\bar{M}}$  from seesaw models of heavy neutrinos, and consistent with the present bounds of Eq. (9), can be obtained considering that the functions  $F_{\text{Box}}$  and  $G_{\text{Box}}$  of Eqs. (11) and (12) are growing functions for large neutrino masses and that the mixings in seesaw models are in general decreasing functions of the neutrino masses. For neutrino masses of a few TeV,  $F_{\text{Box}}$  and  $G_{\text{Box}}$  are of order  $10^1$  and  $10^3$  respectively and we will assume that for those masses the mixings can still be near the maxima shown in Eq. (9). In that case the process is dominated by  $G_{\text{Box}}$  and we obtain

$$G_{M\bar{M}}/G_F \sim \frac{\alpha_W}{32\pi} G_{\text{Box}} \times (s_L^{\nu_\mu})^2 (s_L^{\nu_e})^2 \sim 10^{-6} \quad (14)$$

which is 3 orders of magnitude smaller than present observable values.

If we want to search for larger possible values for  $G_{M\bar{M}}$ , we should assume larger masses for the heavy neutrinos. However, the assumption of larger masses may enter into conflict with the choice of mixing parameters at their current upper bounds [Eq. (9)]. As mentioned earlier, in seesaw models the mixings decrease as the neutrino masses are taken to be larger. If the neutrino masses are very large, the mixings will be forced to be considerably smaller than their current upper bound, and so assuming larger masses may not help to get potentially larger conversion probabilities. This effect was not an issue in Ref. [8] because they assumed rather large Dirac lepton masses ( $m_D \sim M_W$ ). With this assumption one naturally predicts rather large conversion probabilities, however enters into conflict somewhere else: the prediction for the light neutrino masses,  $m_\nu \sim m_D^2/M_h \sim 10^2$  MeV, now turns out to be too large. Therefore, one needs to refine these estimates to be consistent with all present bounds. Here we do it by finding the relation between the neutrino masses and the mixings, following the whole process of mass matrix diagonalization from the start within each model. Keeping these consistency conditions, we search for the largest possible values for  $G_{M\bar{M}}$  in the scenarios of models I and II.

### A. Maximal conversion amplitude in Model I

The key problem is to find the neutrino mass matrix  $\mathcal{M}$  in Eq. (A5) and the mixing parameters  $B_{li}$  in Eq. (A8), constrained by Eq. (9), that maximize the effective coupling  $G_{M\bar{M}}$ .

The general form of  $\mathcal{M}$  for two families in Model I can be described as:

$$\mathcal{M} = \begin{pmatrix} 0 & m_D \\ m_D^T & m_M \end{pmatrix}, \quad m_D = \begin{pmatrix} a & b e^{i\delta_1} \\ c e^{i\delta_2} & d \end{pmatrix}, \quad m_M = \begin{pmatrix} M_1 & 0 \\ 0 & M_2 \end{pmatrix}, \quad (15)$$

where  $a, b, c, d$  are real Dirac masses,  $\delta_j$  ( $j = 1, 2$ ) are two independent physical phases, and  $M_1$  and  $M_2$  (with  $M_1 < M_2$ ) are large masses. The mixing parameters  $B_{li}$  are related to the transformation matrix  $U$  of Eq. (A6), which can be written approximately as a product of a seesaw block matrix  $U_s$  and a light-sector mixing matrix  $V^\dagger$

$$U = V^\dagger U_s, \quad U_s = \begin{bmatrix} (I_{2 \times 2} - \frac{1}{2} m_D m_M^{-2} m_D^\dagger) & -m_D m_M^{-1} \\ m_M^{-1} m_D^\dagger & (I_{2 \times 2} - \frac{1}{2} m_M^{-1} m_D^T m_D m_M^{-1}) \end{bmatrix}, \quad (16)$$

$$V^\dagger = \begin{bmatrix} V_l^\dagger & 0 \\ 0 & I_{2 \times 2} \end{bmatrix}, \quad V_l^\dagger = \begin{pmatrix} \cos \theta & \sin \theta e^{-i\varepsilon} \\ -\sin \theta e^{i\varepsilon} & \cos \theta \end{pmatrix}, \quad (17)$$

where  $\varepsilon$  is a CP phase. The transformation (A6) with  $U_s$  alone gives an approximately block-diagonal mass matrix if we neglect the correction terms  $\mathcal{O}(m_D^2/m_M^2)$  and  $\mathcal{O}(m_D^3/m_M^2)$ :

$$U_s \mathcal{M} U_s^T = \begin{bmatrix} -m_D m_M^{-1} m_D^T (1 + \mathcal{O}(m_D^2/m_M^2)) & \mathcal{O}(m_D^3/m_M^2) \\ \mathcal{O}(m_D^3/m_M^2) & m_M (1 + \mathcal{O}(m_D^2/m_M^2)) \end{bmatrix}. \quad (18)$$

The matrix  $V_l^\dagger$ , Eq. (17), then generates a congruent diagonalization of the light-sector matrix  $m_D m_M^{-1} m_D^T$ . In  $V_l^\dagger$ ,  $\theta = 0$  and  $\pi/4$  correspond to zero and maximal  $\nu_e$ - $\nu_\mu$  mixing. According to solar neutrino experiments, we have maximal  $\nu_e$ - $\nu_\mu$  mixing,  $\theta = \pi/4$ . If we demand that this maximal mixing be obtained independently of the large masses  $M_1$  and  $M_2$ , then straightforward algebra gives the following simple restrictions on the light Dirac sector parameters:

$$a^2 = c^2, \quad b^2 = d^2, \quad \delta_1 = \delta_2 (\equiv \delta). \quad (19)$$

The value of  $\delta$  can be restricted to  $-\pi/2 < \delta \leq \pi/2$ . The two light neutrino eigenmasses are then

$$m_{\nu_e, \nu_\mu} = \left| \left[ \left( \frac{a^2}{M_1} \right)^2 + \left( \frac{b^2}{M_2} \right)^2 + 2 \frac{a^2}{M_1} \frac{b^2}{M_2} \cos(2\delta) \right]^{1/2} \pm \left( \frac{ac}{M_1} + \frac{bd}{M_2} \right) \right|, \quad (20)$$

and the heavy-to-light mixing parameters  $(s_L^{\nu_l})^2 \equiv \sum_{h=3}^4 |B_{lh}|^2$  and  $B_{lh}^* = U_{hl}$  are

$$(s_L^{\nu_e})^2 = (s_L^{\nu_\mu})^2 = \frac{a^2}{M_1^2} + \frac{b^2}{M_2^2} (\equiv s_L^2 < 0.002), \quad (21)$$

$$B_{lh}^* = \begin{bmatrix} a/M_1, & (b/M_2)e^{-i\delta} \\ (c/M_1)e^{-i\delta}, & d/M_2 \end{bmatrix} \quad \ell = e, \mu; \quad h = 3, 4 \quad (22)$$

The elements of the diagonal matrix  $\Lambda$  of Eq. (A6) generally are complex phase factors; here we have  $\lambda_3 = \lambda_4 = +1$  while  $\lambda_1, \lambda_2 \neq +1$ .

In order to reduce the parameter space, for every given  $M_1$  and  $M_2$  we choose the values of the Dirac sector parameters  $(a, b, c, d, \delta_1, \delta_2)$  that maximize the effective coupling  $|G_{M\bar{M}}|$  [Eq. (13)], and then explore the  $M_1, M_2$  parameter space on top of that condition. On the basis of Eq. (13), we can set an upper bound on  $|G_{M\bar{M}}|$ , for given  $M_1$  and  $M_2$ :

$$G_{M\bar{M}}/G_F \leq \frac{\alpha_W}{32\pi} \left\{ \hat{F}_{\text{Box}} \times \left( \sum_{I=3}^4 |B_{eI}^* B_{\mu I}| \right)^2 + \hat{G}_{\text{Box}} \times \sum_{I=3}^4 |B_{eI}^*|^2 \sum_{J=3}^4 |B_{\mu J}|^2 \right\} \quad (23)$$

$$\begin{aligned} &\leq \frac{\alpha_W}{32\pi} (\hat{F}_{\text{Box}} + \hat{G}_{\text{Box}}) \times \sum_{I=3}^4 |B_{eI}^*|^2 \sum_{J=3}^4 |B_{\mu J}|^2 \\ &\leq \frac{\alpha_W}{32\pi} (\hat{F}_{\text{Box}} + \hat{G}_{\text{Box}}) \times (s_L^{\nu_e})^2 (s_L^{\nu_\mu})^2, \end{aligned} \quad (24)$$

where  $\hat{F}_{\text{Box}} = 2 \max |F_{\text{Box}}(x_I, x_J) - 2F_{\text{Box}}(x_I, 0) + F_{\text{Box}}(0, 0)|$ , and  $\hat{G}_{\text{Box}} = \max |G_{\text{Box}}(x_I, x_J)|$ . The maximum of  $G_{M\bar{M}}$  is reached as it approaches this upper bound and simultaneously the maximal values  $(s_L^{\nu_e})^2 = (s_L^{\nu_\mu})^2 = (s_L)_{\text{max}}^2 = 0.002$ , Eqs. (9) and (21), are reached.

Now, there are two distinct cases into which the maximum mixing condition (19) can be divided:

- **Case (a):**  $c = \pm a$  and  $d = \pm b$  (and  $\delta_1 = \delta_2 \equiv \delta$ ). In this case,  $m_{\nu_\mu} \geq (a^2/M_1 + b^2/M_2)$  by Eq. (20), and by Eq. (21) consequently  $s_L^2 \leq m_{\nu_\mu}/M_1 \leq 3 \cdot 10^{-11}$ , where the latter inequality was obtained by taking  $M_1 \geq 100$  GeV and  $m_{\nu_\mu} < 3$  eV as suggested by present neutrino experiments ( $m_{\nu_e} < 3$  eV, Ref. [22];  $\Delta m_{\text{sol}}^2 = |m_{\nu_\mu}^2 - m_{\nu_e}^2| \sim 10^{-10}$  eV<sup>2</sup>  $\approx 0$ , Refs. [23]). This value of  $s_L^2$  extremely suppresses  $G_{M\bar{M}}$ , as seen by Eq. (24), so we will disregard this case for our purposes.
- **Case (b):**  $c = \pm a$  and  $d = \mp b$  (and  $\delta_1 = \delta_2 \equiv \delta$ ). In this case, by Eq. (20)

$$m_{\nu_e, \nu_\mu} = \left| \left[ \left( \frac{a^2}{M_1} \right)^2 + \left( \frac{b^2}{M_2} \right)^2 + 2 \frac{a^2}{M_1} \frac{b^2}{M_2} \cos(2\delta) \right]^{1/2} \pm \left| \frac{a^2}{M_1} - \frac{b^2}{M_2} \right| \right|. \quad (25)$$

Therefore,  $\Delta m_{\text{sol}}^2 = m_{\nu_\mu}^2 - m_{\nu_e}^2 \geq 4|a^2/M_1 - b^2/M_2|^2$ , i.e.,  $|a^2/M_1 - b^2/M_2| \leq (1/2)(\Delta m_{\text{sol}}^2)^{1/2} \sim 10^{-5}$  eV, which is very small compared to  $m_e, m_\mu$ . This means that solar neutrino experiments imply an almost exact relation:

$$a^2/M_1 = b^2/M_2, \quad (26)$$

which in turn implies the following expression for the  $\nu_\mu$  mass:

$$m_{\nu_\mu}/M_1 = (a^2/M_1^2)\sqrt{2(1+\cos 2\delta)}. \quad (27)$$

This is a very small quantity, of order  $10^{-11}$ . Here we see the typical behavior of seesaw models: since  $m_\nu/M_1 \sim a^2/M_1^2$  and the mixing of heavy-to-light sectors is  $B_{\ell h} \sim a/M_1$ , the latter vanishes as the disparity between light vs. heavy neutrino masses intensifies, namely  $m_\nu \ll M_1$ .

However, we do not want  $a/M_1$  to be too small, because it would suppress the mixing parameter  $s_L^2$  [see Eq. (21)]. Therefore, in view of Eq. (27) we set  $\delta \rightarrow \pi/2$ , which keeps the mass disparity without the vanishing of mixing. This is a rather finely tuned condition, but we admit it because we are only looking for maximal transition probabilities. Then, using (21), (26) and the defining condition of this case, namely  $c = a$  and  $d = -b$ , we have set all the parameters of the Dirac sector for maximal conversion probability in terms of just  $M_1$  and  $M_2$ :

$$a = c = M_1(s_L)_{\max}/\sqrt{1+M_1/M_2}, \quad b = -d = a\sqrt{M_2/M_1}, \quad \delta \rightarrow \pi/2. \quad (28)$$

We then proceed to scan the values of  $|G_{M\bar{M}}|$  as a function of  $M_1$  and  $M_2$  restricted to the conditions of Eq. (28). We find, interesting enough, that the Majorana boxes, *i.e.* terms proportional to  $G_{\text{Box}}(x_I, x_J)$ , do not dominate the amplitude for large masses—at least not under condition (28)—even though the functions  $G_{\text{Box}}(x_I, x_J)$  are individually larger than  $F_{\text{Box}}(x_I, x_J)$ . Instead, the mixing elements  $B_{\ell h}$  that multiply these functions are such that both  $F_{\text{Box}}$  and  $G_{\text{Box}}$  terms are of the same order and interfere. Indeed, if one expands the functions  $F_{\text{Box}}$  and  $G_{\text{Box}}$  in the amplitude (13) for asymptotic values of  $x_I$  and  $x_J$ , the leading terms come naïvely from  $G_{\text{Box}}$ ; however, these are multiplied by a factor proportional to  $(m_{\nu_\mu}/M_1)^2$  arising from the mixing elements, which totally suppress them, leaving the leading terms of  $F_{\text{Box}}$  and the subleading terms of  $G_{\text{Box}}$  at the same level of interference.

Fig. 3 shows the graphs for the maximal coupling  $|G_{M\bar{M}}|$  as a function of  $M_1$  and  $M_2$ , which is consistent with all present constraints within model I.

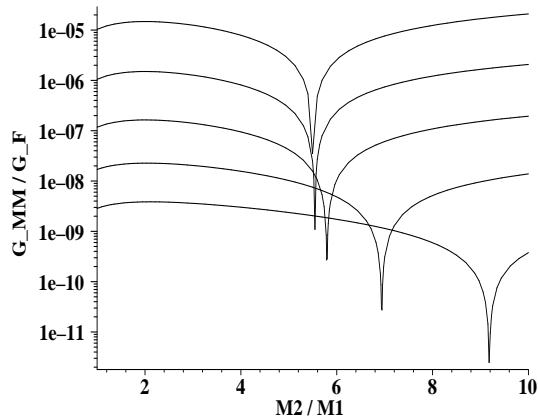


FIG. 3: Maximal effective coupling  $G_{M\bar{M}}/G_F$  for muonium to antimuonium conversion in Model I, as a function of the ratio of Majorana masses  $M_2/M_1$ , for different masses  $M_1$ : from the lower to the upper curve,  $M_1 = 100$  GeV, 300 GeV, 1 TeV, 3 TeV, 10 TeV. The dips reflect an accidental cancellation of the leading terms of Dirac and Majorana box diagrams for particular values of  $M_1$  and  $M_2$ .

We see that the amplitude is indeed a growing function of  $M_1, M_2$  (we also see that for given  $M_1$ , local maxima are reached if  $M_2 \approx 2M_1$ ). We do not push  $M_1, M_2$  higher than around 10 TeV, because the perturbative expansion to one loop breaks down above that scale, as the authors of Ref. [12] point out. They stated that the perturbative expansion is valid provided  $M_h^2 \sum_\ell |B_{\ell h}|^2 < 2M_W^2/\alpha_W$ . In our case, this condition becomes:

$$M_1 M_2 < \frac{M_W^2}{\alpha_W s_L^2} \sim (10 \text{ TeV})^2. \quad (29)$$

From Fig. 3, we see that the maximum expected value of  $G_{M\bar{M}}/G_F$  is around  $10^{-5} \rightarrow 10_4$ , which is still almost two orders of magnitude below the level of sensitivity of current experiments. To close the analysis, we may comment on the finely tuned parameter  $\delta \rightarrow \pi/2$ . It is clear that if we do not impose this condition, then the mixing elements  $s_L^2$  are  $\sim a^2/M_1^2 \sim m_\nu/M_1$ . For  $m_{\nu_\mu} \sim 190$  KeV, which is the upper bound [22], and  $M_1 \sim 10$  TeV, we get  $s_L^2 \sim 10^{-8}$ , which signifies a suppression of 6 orders of magnitude in the amplitude with respect to the maxima found in our analysis.

### B. Maximal conversion amplitude in Model II

In Model II, Eq. (A12), with CP-conserving mass terms, the submatrices are real and can be taken in the form

$$\mathcal{M} = \begin{pmatrix} 0 & m_D & 0 \\ m_D^T & 0 & m_M^T \\ 0 & m_M & 0 \end{pmatrix}, \quad m_D = \begin{pmatrix} a & b \\ c & d \end{pmatrix}, \quad m_M = \begin{pmatrix} M_1 & 0 \\ 0 & M_2 \end{pmatrix}. \quad (30)$$

Again here  $M_1$  and  $M_2$  ( $M_1 \leq M_2$ ) are of the order of the heavy Majorana masses, and  $a, b, c, d \sim M_j |s_L^{\nu_l}|$ . By diagonalization of matrix  $\mathcal{M}$  [see Eq. (A6), but this time with  $U$  orthogonal] we get the neutrino masses

$$\begin{aligned} m_1 &= m_2 = 0, \\ m_3 &= m_4 = M_1 \left[ 1 + \frac{1}{2} \frac{a^2 + c^2}{M_1^2} + \dots \right], \\ m_5 &= m_6 = M_2 \left[ 1 + \frac{1}{2} \frac{b^2 + d^2}{M_2^2} + \dots \right], \end{aligned} \quad (31)$$

where the dots represent terms  $\sim 1/M_j^4$ . The phase factors in Eq. (A6) are  $\lambda_3 = \lambda_5 = -1$ ,  $\lambda_1 = \lambda_2 = \lambda_4 = \lambda_6 = +1$  and the mixing elements  $B_{lh}$  are real, fulfill the symmetry  $B_{l3} = B_{l4}$  and  $B_{l5} = B_{l6}$  (for  $l = e, \mu$ ), and are given explicitly by:

$$B_{lh} = \frac{1}{\sqrt{2}} \begin{bmatrix} -a/M_1, & -a/M_1, & b/M_2, & b/M_2 \\ -c/M_1, & -c/M_1, & d/M_2, & d/M_2 \end{bmatrix} + \mathcal{O}(m_D^3/m_M^3) \dots, \quad \ell = e, \mu; \quad h = 3, 4, 5, 6 \quad (32)$$

Notice that the two ‘‘light’’ neutrinos are actually massless, although they can easily acquire small masses by introducing small nonzero entries in the lower right  $2 \times 2$  block of the mass matrix  $\mathcal{M}$ . The two degenerate pairs of heavy Majorana neutrinos can be interpreted as two heavy Dirac neutrinos. The symmetry in the masses, mixings and phase factors imply that the contribution to  $G_{M\bar{M}}$  from the Majorana boxes of Fig. 2, [*i.e.* the terms with  $G_{\text{Box}}(x_I, x_J)$  in Eq. 13], cancel out. This contrasts with Model I where such terms are important, and it is related to the fact that Model II conserves total lepton *number* while Model I does not.

As before, we search for the maximum of  $|G_{M\bar{M}}/G_F|$ . Since the  $G_{\text{Box}}(x_I, x_J)$  terms cancel, and the mixing elements  $B_{lh}$  are real in absence of CP violation, we can write

$$\begin{aligned} |G_{M\bar{M}}/G_F| &= \frac{\alpha_W}{32\pi} \times \left| \sum_{I,J=3}^6 \left\{ 2B_{eI}B_{eJ}B_{\mu I}B_{\mu J} [F_{\text{Box}}(x_I, x_J) - 2F_{\text{Box}}(x_I, 0) + F_{\text{Box}}(0, 0)] \right\} \right| \\ &\leq \frac{\alpha_W}{32\pi} \hat{F}_{\text{Box}} \left( \sum_{I=3}^6 B_{eI}B_{\mu I} \right)^2. \\ &\leq \frac{\alpha_W}{32\pi} \hat{F}_{\text{Box}} (s_L^{\nu_e})^2 (s_L^{\nu_\mu})^2, \end{aligned} \quad (33)$$

where  $\hat{F}_{\text{Box}} = 2\max|F_{\text{Box}}(x_I, x_J) - 2F_{\text{Box}}(x_I, 0) + F_{\text{Box}}(0, 0)|$ . The last inequality is Schwarz’s inequality, which saturates when the following proportionalities are reached:

$$\frac{B_{e3}}{B_{\mu3}} = \frac{B_{e4}}{B_{\mu4}} = \frac{B_{e5}}{B_{\mu5}} = \frac{B_{e6}}{B_{\mu6}}. \quad (34)$$

The first and the third equalities are fulfilled automatically. The second equality, however, can be shown to be fulfilled only when  $ad = bc$ . Thus, the maximum of  $|G_{M\bar{M}}|$  is reached when  $(s_L^{\nu_e})^2$  and  $(s_L^{\nu_\mu})^2$  are at their upper bounds,



Eqs. (9)

$$(s_L^{\nu_e})^2 = \frac{a^2}{M_1^2} + \frac{b^2}{M_2^2} + \mathcal{O}(m_D^4/m_M^4) = 0.005, \quad (35)$$

$$(s_L^{\nu_\mu})^2 = \frac{c^2}{M_1^2} + \frac{d^2}{M_2^2} + \mathcal{O}(m_D^4/m_M^4) = 0.002, \quad (36)$$

and the condition  $ad = bc$  is simultaneously fulfilled. This implies, for given values of high mass parameters  $M_1$  and  $M_2$ , three relations for the four low mass parameters  $a$ ,  $b$ ,  $c$  and  $d$ . Thus, we still have one degree of freedom for fixing the values of low mass parameters, without much effect on the conversion probability. The simplest additional relation seems to be the symmetry assumption  $b = c$ . All this then gives the optimal choice of low mass parameters  $a$ ,  $b$ ,  $c$  and  $d$  in Model II:

$$a = \frac{M_2}{\sqrt{(M_2/M_1)^2 + (s_L^{\nu_\mu}/s_L^{\nu_e})^2}} \frac{s_L^{\nu_e}}{\sqrt{1 - s_L^{\nu_e 2} - s_L^{\nu_\mu 2}}}, \quad (37)$$

$$b = c = a \times (s_L^{\nu_\mu}/s_L^{\nu_e}), \quad d = a \times (s_L^{\nu_\mu}/s_L^{\nu_e})^2, \quad (38)$$

where  $s_L^{\nu_e}$  and  $s_L^{\nu_\mu}$  are taken at their respective upper bound. Again, we have reduced the parameter space to just two quantities,  $M_1$  and  $M_2$ . Fig. 4 shows the graphs for the maximal effective coupling  $|G_{M\bar{M}}|$  as a function of  $M_1$  and  $M_2$ , which is consistent with all present constraints within model II.

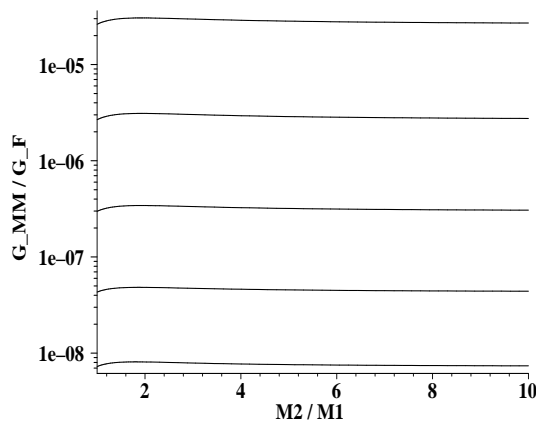


FIG. 4: Maximal effective coupling  $G_{M\bar{M}}/G_F$  for muonium to antimuonium conversion in Model II, as a function of the ratio of Majorana masses  $M_2/M_1$ , for different masses  $M_1$ : from the lower to the upper curve,  $M_1 = 100$  GeV, 300 GeV, 1 TeV, 3 TeV, 10 TeV.

We see that in this model the amplitude  $G_{M\bar{M}}$  is an increasing function of  $M_1$ , but is rather insensitive to  $M_2$  ( $M_2 > M_1$  by definition). Comparing Figs. 3 and 4 we see that in model II the maximum probability can reach slightly larger values than in model I. However, there is a stronger distinction between the models: here the maxima are reached for natural values of the parameters, while the maxima in model I are only reached for a finely tuned condition, which circumvents the seesaw suppression of the mixing; away from this finely tuned condition, the mixing suppression is very strong, pushing the amplitude of model I several orders of magnitude below the maximum.

#### IV. PROSPECTS FOR FREE $e^- \mu^+ \rightarrow \mu^- e^+$ COLLISIONS

As an aside from this calculation, one can notice that the same amplitude obtained from the box diagrams can be used to determine the cross section for free  $e^- \mu^+ \rightarrow \mu^- e^+$  collisions. The result is simply:

$$\begin{aligned} \sigma(e^- \mu^+ \rightarrow \mu^- e^+) &= \frac{4\pi}{3} \frac{\alpha_w^2}{M_W^4} s |G_{M\bar{M}}/G_F|^2 \\ &\sim 3 \times 10^{-5} \left( \frac{s}{M_W^2} \right) \left( \frac{|G_{M\bar{M}}|/G_F}{10^{-5}} \right)^2 \text{ fbarn.} \end{aligned} \quad (39)$$

This expression is applicable for CMS energies well above  $m_\mu$  but below  $M_W$ , i.e., for  $1 \text{ GeV} < \sqrt{s} < 10^2 \text{ GeV}$ . In this kinematical regime, the cross section is clearly too small to be observed in the foreseeable future, especially considering that both expressions in parentheses are at most of order unity. For this reason, we will comment on this process no further.

#### V. CONCLUSIONS

We have looked for the maximum probabilities of muonium to antimuonium conversion that can be reached in models where the required lepton flavor violation is caused by heavy neutrinos, keeping consistency with all present bounds. The estimates are done within two alternative models. In both models the amplitudes are in general growing functions of the heavy neutrino masses. Our estimates of the amplitudes are thus limited by two effects: (i) suppression of flavor mixing matrix elements as the masses get larger and (ii) the breakdown of perturbative expansion for masses above a few tens of TeV.

Model I includes extra right handed neutrino singlets and constitutes a typical seesaw model for the neutrino masses and mixings, which violates lepton flavor as well as lepton number. Model II includes extra right handed and left handed neutrino singlets in such a way that lepton flavor is violated, yet lepton number is conserved. We found that in Model I the Majorana boxes give the dominant contribution over the Dirac boxes in the most typical scenarios, yet the maximum probabilities are obtained in finely tuned regions of the parameter space, where Dirac and Majorana boxes are comparable and even tend to interfere destructively. As a consequence of this effect, the maximal conversion rates are not as large as one could have naïvely estimated. The maximal couplings thus obtained are  $G_{M\bar{M}}/G_F \sim 10^{-5}$ , which means conversion probabilities 4 orders of magnitude below present experimental sensitivities. Moreover, away from the finely tuned condition, the small masses of the light neutrinos enforce a dramatic suppression of the mixing (a typical seesaw behavior) and the probabilities drop by several orders of magnitude to unreachable levels.

Model II, in contrast, requires no finely tuned condition to reach its maximal amplitudes. In this case, because of lepton number conservation, the heavy Majorana neutrinos come in degenerate pairs, thus acting effectively as Dirac neutrinos. As a result, the Majorana boxes cancel in the amplitudes and the standard Dirac boxes, which are generally smaller, are the only contribution. Therefore, the cancellation of the Majorana boxes occurs only in model II and it is due to interference between the different neutrino flavors (*i.e.* the flavor mixing matrix), and not because of Fermi statistics, as was stated in ref. [8]. Despite the cancellation of the Majorana boxes, Model II gives the largest possible conversion probability, because the mixings are free from the seesaw suppression of model I imposed by the light neutrino masses. Overall, the effective coupling  $G_{M\bar{M}}/G_F$  in model II can reach  $10^{-5} \rightarrow 10^{-4}$  for natural values of the parameters and neutrino masses around 10 TeV.

We also included the calculation of free  $\mu^+ e^- \rightarrow \mu^- e^+$  scattering at high energies, because this process tests the same amplitude as muonium-antimuonium conversion. However the cross section is so small that muonium-antimuonium conversion is still a more hopeful alternative from the experimental point of view.

#### Acknowledgments

C.D. and G.C. are grateful to S. Kovalenko for useful discussions. C.D. acknowledges support from Fondecyt (Chile) research grant No. 1030254 and G.C. from Fondecyt grants No. 1010094 and No. 7010094. The work of C.S.K. was supported in part by the CHEP-SRC Program and by Grant No. R02-2003-000-10050-0 from BRP of the KOSEF (Korea). The work of J.D.K was supported by the Korea Research Foundation Grant (2001-042-D00022).

## APPENDIX A: THE MODELS

In this Appendix we will briefly describe two distinct seesaw-type models, which are used in our numerical evaluation of the muonium-antimuonium conversion probability. Basically, these models have extended neutrino sectors as compared with the SM. The entire lepton sector has the same spectrum as the Standard Model (we consider  $N_L$  families in general) plus  $N_H$  extra right-handed neutrinos  $\tilde{\nu}_R^{(j)}$  ( $j = 1, \dots, N_H$ ). The lepton sector is thus divided in  $N_L$   $SU(2)_L$ -doublets  $L^{(i)}$ ,  $N_L$  charged singlets  $l_R^{(i)}$  and  $N_H$  neutral singlets  $\tilde{\nu}_R^{(j)}$

$$L^{(i)} = \begin{pmatrix} \nu_L^{(i)} \\ l_L^{(i)} \end{pmatrix}, \quad l_R^{(i)}, \quad \tilde{\nu}_R^{(j)}, \quad (i = 1, \dots, N_L; j = 1, \dots, N_H). \quad (\text{A1})$$

Concerning the interactions, only those involving charged currents are relevant to our case (lepton currents coupled to  $W$ 's and, in a general gauge, to charged Goldstone bosons  $G^\pm$ ):

$$\mathcal{L}_{lnW}(x) = \left( -\frac{g}{\sqrt{2}} \right) [\bar{l}(x)\gamma_\mu\nu_L(x)] W^-(x)^\mu + \text{h.c.}, \quad (\text{A2})$$

$$\mathcal{L}_{lnG}(x) = \left( -\frac{g}{\sqrt{2}M_W} \right) G^-(x) [\bar{l}(x)m_l^\dagger\nu_L(x) - \bar{l}(x)m_D\tilde{\nu}_R(x)] + \text{h.c.} \quad (\text{A3})$$

In Eqs. (A2)-(A3), we used the following simplified notation:  $l$  is a column with the  $N_L$  charged leptons,  $l_i = l_L^{(i)} + l_R^{(i)}$ ;  $\nu_L$  is a column with the  $N_L$  standard neutrinos,  $\nu_L^{(i)}$ ;  $\tilde{\nu}_R$  is a column with the  $N_H$  extra neutrinos  $\tilde{\nu}_R^{(j)}$ ;  $m_l$  is the standard  $N_L \times N_L$  mass matrix of the charged leptons (which can be taken to be diagonal and positive, without loss of generality);  $m_D$  is a new  $N_L \times N_H$  mass matrix of Dirac type for the neutrinos.  $g$  is the  $SU(2)_L$  coupling constant ( $g^2 = 8G_F M_W^2 / \sqrt{2}$ ).

Expression (A3) is obtained from the Yukawa terms for the leptons and the Higgs doublet  $\Phi$  (or its conjugate  $\Phi^c = i\tau_2\Phi^*$ ):

$$\mathcal{L}_Y(x) = \sum_{i,j=1}^{N_L} \bar{L}^{(i)}(x) \Phi(x) (-\mathcal{D}_{ij}) l_R^{(j)}(x) + \sum_{j=1}^{N_H} \sum_{i=1}^{N_L} \bar{L}^{(i)}(x) \Phi^c(x) (-\mathcal{U}_{ij}) \tilde{\nu}_R^{(j)}(x) + \text{h.c.} \quad (\text{A4})$$

The first term is standard and gives the mass to the charged leptons in terms of the Yukawa couplings  $\mathcal{D}_{ij}$  when the Higgs acquires a vev  $\langle \Phi \rangle = (0, v)^T / \sqrt{2}$ , namely  $[m_l]_{ij} = \mathcal{D}_{ij} v / \sqrt{2}$ ; it also generates the first interaction term in Eq. (A3). The second term is extra physics; in a similar way it generates Dirac type masses for the neutrinos,  $[m_D]_{ij} = \mathcal{U}_{ij} v / \sqrt{2}$  and the second interaction term in Eq. (A3).

In addition, in these seesaw models there are neutrino mass terms of Majorana type,  $\propto \overline{\tilde{\nu}_R^c} \tilde{\nu}_R + \text{h.c.}$ , which can be gathered in a matrix  $m_M$  of dimension  $N_H \times N_H$ . Consequently, the totality of neutrino mass terms can be expressed in the form:

$$-\mathcal{L}_{\text{mass}}^\nu = \frac{1}{2} \left( \overline{\nu_L}, \overline{\tilde{\nu}_R^c} \right) \mathcal{M} \begin{pmatrix} \nu_L^c \\ \tilde{\nu}_R \end{pmatrix} + \text{h.c.} = \frac{1}{2} \left( \overline{\nu_L}, \overline{\tilde{\nu}_R^c} \right) \begin{pmatrix} 0 & m_D \\ m_D^T & m_M \end{pmatrix} \begin{pmatrix} \nu_L^c \\ \tilde{\nu}_R \end{pmatrix} + \text{h.c.} \quad (\text{A5})$$

The superscript ‘‘c’’ denotes charge-conjugated fields  $\psi^c = \mathcal{C}\bar{\psi}^T$ , where  $\mathcal{C} = -i\gamma^2\gamma^0$  in the Dirac representation. The block in the upper left corner is zero due to the  $\rho$ -parameter constraints (see e.g. Ref. [14]). The total mass matrix  $\mathcal{M}$  appearing in Eq. (A5) has dimension  $(N_L + N_H) \times (N_L + N_H)$  and is a symmetric, in general complex, matrix with a texture leading to a seesaw mechanism upon diagonalization. This matrix can always be diagonalized by means of a congruent transformation involving a unitary matrix  $U$  [15]

$$U\mathcal{M}U^T\Lambda^* = \mathcal{M}_d. \quad (\text{A6})$$

Here,  $\mathcal{M}_d$  is a nonnegative diagonal matrix, and  $\Lambda^*$  is a diagonal unitary matrix:  $(\Lambda^*)_{ij} = \delta_{ij}\lambda_i^*$ , where  $\lambda_i$  are complex phase factors ( $|\lambda_i| = 1$ ) such that  $\mathcal{M}_d$  is made real and nonnegative. The diagonal  $\Lambda^*$  matrix in Eq. (A6) can be incorporated into  $U$  by the redefinition:  $U_{\text{new}} = (\Lambda^*)^{1/2}U$ , where  $U_{\text{new}}$  is again unitary;  $\Lambda^*$  thus reflects a freedom of choice for  $U$ . The  $N_L + N_H$  mass eigenstates  $n_i$  are Majorana neutrinos, related to the interaction eigenstates  $\nu_a$  by the matrix  $U$  of Eq. (A6)

$$\begin{pmatrix} \nu_L \\ \tilde{\nu}_R^c \end{pmatrix}_a = \sum_{i=1}^{N_L+N_H} U_{ia}^* n_{iL} \quad \Rightarrow \quad \begin{pmatrix} \nu_L^c \\ \tilde{\nu}_R \end{pmatrix}_a = \sum_{i=1}^{N_L+N_H} U_{ia} \lambda_i^* n_{iR}, \quad (\text{A7})$$

The first  $N_L$  mass eigenstates are the light standard partners of the charged leptons, while the other  $N_H$  eigenstates are heavy (if the seesaw mechanism takes place). The factor  $(\Lambda^*)_{ii} = \lambda_i^*$  is now recognized as the creation phase factor [14, 16] of the Majorana neutrino  $n_i$  ( $\equiv n_{iL} + n_{iR}$ ), in the sense that  $n_i^c = \lambda_i^* n_i$ , and more specifically  $(n_{iL})^c = \lambda_i^* n_{iR}$ . The  $N_L \times (N_L + N_H)$ -dimensional mixing matrix  $B$  for charged current interactions is defined as

$$B_{li} = U_{il}^* = (U^\dagger)_{li} . \quad (\text{A8})$$

When CP is conserved, the coefficients  $B_{li}$  can be chosen real and all the phase factors  $\lambda_i$  real as well [14]:  $\lambda_i = \tilde{\eta}_{\text{CP}}(n_i)/i = \pm 1$ , where  $\tilde{\eta}_{\text{CP}}(n_i) = \pm i$  is the intrinsic CP parity of the Majorana neutrino  $n_i$ . If the symmetric mass matrix  $\mathcal{M}$  is real, then there exists a unitary real (i.e., orthogonal) matrix  $U = \mathcal{O}$  such that

$$\mathcal{O}\mathcal{M}\mathcal{O}^T = \mathcal{D} , \quad (\text{A9})$$

where  $\mathcal{D}$  is a diagonal and real matrix; in general, some of its diagonal elements are negative, but the absolute values are the same as those of  $\mathcal{M}_d = \mathcal{D}\Lambda^*$ :  $(\mathcal{M}_d)_{ii} = \mathcal{D}_{ii}\lambda_i^* = |\mathcal{D}_{ii}|$ . We see that  $\lambda_i$  is here  $\pm 1$  ( $= \text{sgn}[\mathcal{D}_{ii}]$ ). Therefore, when the symmetric mass matrix  $\mathcal{M}$  is real, we are in a situation with no CP violation:  $B_{li} = \mathcal{O}_{il}$  are real, and  $\lambda_i = \pm 1$ . Even more, in that case  $\mathcal{O}_{ij}$  for  $j > N_L$  are also real. Thus, the reality of  $\mathcal{M}$  is sufficient for having CP conservation.<sup>1</sup> We will see later that in this case the values of  $\lambda_i$  either as  $+1$  or  $-1$ , separately for each  $i$  ( $i = 1, \dots, N_L + N_H$ ), influence our results.

Inserting the transformations (A7) in the interaction terms (A2) and (A3), taking also into account the mass matrix form (A5) and the transformation (A6) into Eq. (A3), we obtain the explicit interactions of the charged bosons with the leptons in their mass basis:

$$\mathcal{L}_{lnW}(x) = \left( -\frac{g}{\sqrt{2}} \right) \sum_{i=1}^{N_L} \sum_{j=1}^{N_L+N_H} [B_{ij}\bar{l}_i(x)\gamma_\mu P_L n_j(x)] W^-(x)^\mu + \text{h.c.} , \quad (\text{A10})$$

$$\mathcal{L}_{lnG}(x) = \left( -\frac{g}{\sqrt{2}M_W} \right) G^-(x) \sum_{i=1}^{N_L} \sum_{j=1}^{N_L+N_H} [B_{ij}\bar{l}_i(x)(m_i P_L - M_j P_R) n_j(x)] + \text{h.c.} , \quad (\text{A11})$$

where  $m_i > 0$  is the mass of the charged lepton  $l_i$ , and  $M_j \geq 0$  the mass of the Majorana neutrino  $n_j$ . Expressions (A10) and (A11) were obtained already in Ref. [17], and used in Refs. [6, 12] and others.

In this work, we have used two specific models:

**Model I:** This is the usual seesaw model described above, with  $N_L$  left-handed neutrinos  $\nu_{iL}$  and an equal number of right-handed neutrinos  $\tilde{\nu}_{iR}$ :  $N_H = N_L$ . The neutrino mass terms are those given in Eq. (A5). The square ( $N_L \times N_L$ ) matrices  $m_M$  and  $m_D$  are supposed to be invertible.

The heavy-to-light neutrino mixings  $(s_L^\nu)^2 \equiv \sum_h |U_{hi}|^2$  are of the order of the squared ratio between the Dirac mass ( $m_D$ ) and the Majorana mass ( $m_M$ ) scales ( $\sim |m_D|^2/|m_M|^2$ ). The eigenmasses of the light neutrinos are  $m_{\nu_{light}} \sim m_D^2/m_M$ . Severe constraints on the  $|m_D| \ll |m_M|$  hierarchy in Model I are imposed by the very low experimental bounds  $m_{\nu_{light}} \lesssim 1$  eV. Another set of constraints on the model is imposed by the present experimental bounds on the heavy-to-light mixing parameters  $(s_L^\nu)^2 \sim |m_D|^2/|m_M|^2$  ( $\lesssim 10^{-2}$ , see below).

**Model II:** This model is formally again of the seesaw type, because the mass matrix  $\mathcal{M}$  has a form similar to (A5). However, now  $N_H = 2N_L$ . This model contains an equal number  $N_L$  of left-handed ( $S_{iL}$ ) and right-handed ( $\tilde{\nu}_{iR}$ ) neutral singlets [18, 19], and thus the right-handed column  $\tilde{\nu}_R$  with  $N_H$  components is now  $(\tilde{\nu}_R, S_L^c)^T$ . The form of the mass matrix  $\mathcal{M}$  in this model ensures conservation of total lepton number, but lepton flavor mixing is still possible. The neutrino mass terms, after electroweak symmetry breaking, have the form

$$-\mathcal{L}_{\text{mass}}^\nu = \frac{1}{2} \left( \overline{\nu}_L, \overline{\tilde{\nu}_R^c}, \overline{S}_L \right) \mathcal{M} \begin{pmatrix} \nu_L^c \\ \tilde{\nu}_R \\ S_L^c \end{pmatrix} + \text{h.c.} , \quad \mathcal{M} = \begin{pmatrix} 0 & m_D & 0 \\ m_D^T & 0 & m_M^T \\ 0 & m_M & 0 \end{pmatrix} , \quad (\text{A12})$$

which is formally of the form (A5), but with a specific  $N_L \times N_L$  texture: the Dirac mass submatrix now has a specific  $N_L \times 2N_L$  form  $(m_D, 0)$ , where  $m_D$  is a square ( $N_L \times N_L$ ) matrix, and 0 is the  $N_L \times N_L$  zero matrix; and the Majorana

<sup>1</sup> It is not clear to us what are the necessary and sufficient conditions on the elements of  $\mathcal{M}$  for having CP conservation. If only the upper left  $N_L \times N_L$  block of  $\mathcal{M}$  is real, it appears that we can have CP violation, i.e., the elements  $B_{li} = U_{il}^*$  ( $l = 1, \dots, N_L$ ) apparently cannot always be chosen real in such a case.

mass submatrix  $m_M$  of (A5) is now replaced by a  $2N_L \times 2N_L$  matrix in the lower right part of  $\mathcal{M}$  (A12). As given in (A12), the matrix  $\mathcal{M}$  gives for each of the  $N_L$  generations a massless Weyl neutrino and two degenerate Majorana neutrinos [20, 21]. Consequently, the seesaw-type restriction  $m_{\nu_{i\text{ght}}} \sim m_D^2/m_M \lesssim 1$  eV of Model I is absent in Model II in its unperturbed form (A12). Nevertheless, the experimental bounds on the heavy-to-light mixing parameters  $(s_L^\nu)^2 \sim |m_D|^2/|m_M|^2$  ( $\lesssim 10^{-2}$ ) do impose a hierarchy  $|m_D| < |m_M|$  between the Dirac and Majorana mass sectors and, in this sense, the model remains of a seesaw type, but the hierarchy  $|m_D| < |m_M|$  here is in general much weaker than in Model I. Interestingly, nonzero masses for the  $N_L$  light neutrinos can easily be included in Model II by introducing small Majorana mass terms for the neutral singlets  $S_{iL}$ , i.e., small nonzero elements in the  $N_L \times N_L$  lower right block of  $\mathcal{M}$ . The mixings of heavy-to-light neutrinos are not significantly affected by these small corrections.

The above two models, for specific choices of the  $N_L \times N_L$  matrices  $m_D$  and  $m_M$ , give us specific values of the mixing-matrix elements (A8) and eigenmasses  $M_j$ , i.e., the parameters which then determine the charge current interactions of (A10) and (A11).

## APPENDIX B: BOX DIAGRAM AMPLITUDES WITH MAJORANA NEUTRINOS

Here we outline the derivation of the expression for  $G_{MM}$  in Eq. (10) at one loop order (box diagrams), defined by the effective lagrangian of Eq. (1).

There are basically four types of box diagrams: two containing generic neutrinos (Fig. 1) and two exclusive for Majorana neutrinos only (Fig. 2). According to the contractions of the fields with the external states, the diagrams of Fig. 1.b, 2.a and 2.b have the same relative sign, while the diagram of Fig. 1.a has the opposite sign.

There are also basically two momentum integrals encountered in the box diagrams, in the limit where external masses and momenta are neglected compared to the loop momenta. The first one is:

$$I_{ij} \equiv \int \frac{d^4q}{(2\pi)^4} \frac{1}{(q^2 - M_i^2)(q^2 - M_j^2)(q^2 - M_W^2)^2} = \frac{i}{(4\pi)^2 M_W^4} \mathcal{J}(x_i, x_j), \quad (\text{B1})$$

where we denote  $x_j = M_j^2/M_W^2$  and where  $\mathcal{J}(x_i, x_j)$  is a dimensionless expression:

$$\mathcal{J}(x_i, x_j) = -\frac{1}{(x_i - x_j)} \left\{ \left( \frac{1}{1 - x_i} + \frac{x_i \ln x_i}{(1 - x_i)^2} \right) - (x_i \rightarrow x_j) \right\}. \quad (\text{B2})$$

The second integral is:

$$K_{ij} \equiv \int \frac{d^4q}{(2\pi)^4} \frac{q^2}{(q^2 - M_i^2)(q^2 - M_j^2)(q^2 - M_W^2)^2} = \frac{i}{(4\pi)^2 M_W^2} \mathcal{K}(x_i, x_j), \quad (\text{B3})$$

where the dimensionless expression is:

$$\mathcal{K}(x_i, x_j) = -\frac{1}{(x_i - x_j)} \left\{ \left( \frac{1}{1 - x_i} + \frac{x_i^2 \ln x_i}{(1 - x_i)^2} \right) - (x_i \rightarrow x_j) \right\}. \quad (\text{B4})$$

The transition amplitudes  $\mathcal{T}_{WW}^{(1a)}$  and  $\mathcal{T}_{WW}^{(1b)}$ , which correspond to the diagrams of Figs. 1.a and 1.b when both internal bosons are  $W$ , are:

$$\begin{aligned} \left\{ \begin{array}{l} \mathcal{T}_{WW}^{(1a)} \\ \mathcal{T}_{WW}^{(1b)} \end{array} \right\} &= \left( -\frac{g}{\sqrt{2}} \right)^4 B_{ei}^* B_{ej}^* B_{\mu i} B_{\mu j} \\ &\times \int \frac{d^4q}{(2\pi)^4} \frac{1}{(q^2 - M_i^2)(q^2 - M_j^2)(q^2 - M_W^2)^2} \left\{ \begin{array}{l} (+1) [\bar{u}(k') \gamma_\mu \not{q} \gamma_\nu P_L v(p')] [\bar{v}(k) \gamma^\nu \not{q} \gamma^\mu P_L u(p)] \\ (-1) [\bar{u}(k') \gamma_\mu \not{q} \gamma_\nu P_L u(p)] [\bar{v}(k) \gamma^\nu \not{q} \gamma^\mu P_L v(p')] \end{array} \right\}. \end{aligned} \quad (\text{B5})$$

Overall we label  $p$  and  $p'$  as the momenta of the initial and final electron (positron), and  $k$  and  $k'$  as the initial and final momenta of the (anti-) muons. To simplify the notation, we have omitted the spin and flavor labels in the spinors, since the momenta specify them unambiguously, (c.f. Fig. 1). We notice a factor  $(-1)$  in the second amplitude; its origin is the anticommutation of the fermion fields involved in the Wick contractions with the external states. Now, using the identity

$$\gamma_\mu \gamma_\alpha \gamma_\nu = i \epsilon_{\lambda\mu\alpha\nu} \gamma^\lambda \gamma_5 + \gamma_\mu g_{\alpha\nu} + \gamma_\nu g_{\mu\alpha} - \gamma_\alpha g_{\mu\nu} \quad (\text{B6})$$

the spinor structure can be simplified to the following form (we have omitted the spinors in the brackets):

$$[\gamma_\mu \not{q} \gamma_\nu P_L] [\gamma^\nu \not{q} \gamma^\mu P_L] = 4q^\alpha q^\beta [\gamma_\alpha P_L] [\gamma_\beta P_L]. \quad (\text{B7})$$

Finally, after replacing  $q^\alpha q^\beta \rightarrow g^{\alpha\beta} q^2/4$  due to the Lorentz invariance of the integrals and doing the following Fierz transformation in the second amplitude:

$$[\bar{u}_1 \gamma_\alpha P_L u_2] [\bar{v}_3 \gamma^\alpha P_L v_4] = -[\bar{u}_1 \gamma_\alpha P_L v_4] [\bar{v}_3 \gamma^\alpha P_L u_2] \quad (\text{B8})$$

both amplitudes in Eq. (B5) become identical:

$$\mathcal{T}_{WW}^{(1a)} = \mathcal{T}_{WW}^{(1b)} = i \frac{\alpha_w^2}{4M_W^2} B_{ei}^* B_{ej}^* B_{\mu i} B_{\mu j} \mathcal{K}(x_i, x_j) [\bar{u}(k') \gamma_\alpha P_L v(p')] [\bar{v}(k) \gamma^\alpha P_L u(p)]. \quad (\text{B9})$$

In the gauge we are using, one must also include the diagrams with one and two Goldstone bosons, *i.e.*  $\mathcal{T}_{WG}^{(1a)}$ ,  $\mathcal{T}_{GW}^{(1a)}$ ,  $\mathcal{T}_{GG}^{(1a)}$ , etc. The calculation goes through similar steps as those already stated for the box with two  $W$ 's, but contains different propagators and therefore different combinations of the integrals (B1) and (B3).

The sum of all these diagrams gives the total amplitude of the ‘‘Dirac’’ box diagrams of Fig. 1:

$$\begin{aligned} \mathcal{T}^{(1)} &\equiv \sum_{\kappa=a,b} \left[ \mathcal{T}_{WW}^{(1\kappa)} + \mathcal{T}_{GG}^{(1\kappa)} + \mathcal{T}_{GW+WG}^{(1\kappa)} \right] \\ &= -i \frac{\alpha_w^2}{4M_W^2} 2B_{ei}^* B_{ej}^* B_{\mu i} B_{\mu j} F_{\text{Box}}(x_i, x_j) [\bar{u}(k') \gamma_\alpha P_L v(p')] [\bar{v}(k) \gamma^\alpha P_L u(p)], \end{aligned} \quad (\text{B10})$$

where  $F_{\text{Box}}(x_i, x_j)$  is given in Eq. (11) and is identical to the expression  $F_{\text{Box}}(x_i, x_j)$  of Ref. [12].

The diagrams of Fig. 2 are, on the other hand, different in the sense that they exist only if the internal neutrinos are of Majorana type. The Wick contractions of the Majorana fields can be performed in the usual way if we previously transform two of the four vertex operators as follows: (we chose the vertices with the initial anti-muon and with the final anti-electron):

$$\bar{\psi}_\mu(x) \gamma_\nu P_L n_j(x) = -\lambda_j \bar{n}_j(x) \gamma_\nu P_R \psi_\mu^c(x), \quad (\text{B11a})$$

$$\bar{n}_i(x) \gamma_\mu P_L \psi_e(x) = -\lambda_i^* \bar{\psi}_e^c(x) \gamma_\mu P_R n_i(x). \quad (\text{B11b})$$

Here,  $\lambda_j$  is the creation phase factor of the Majorana neutrino  $n_j$ , *i.e.*  $n_j^c = \lambda_j^* n_j$ , and the superscript ‘‘c’’ denotes the conjugated field  $\psi^c = \mathcal{C} \bar{\psi}^T$ , where  $\mathcal{C} = -i\gamma^2 \gamma^0$  in the Dirac representation. After performing the transformations (B11), we can contract the  $\bar{n}(x_k)$ 's and  $n(x_n)$ 's into normal neutrino propagators (see Ref. [14]). Let us first consider the two diagrams of Fig. 2 with two internal  $W$ 's. These diagrams differ from each other only in the way the  $W$ 's are contracted. The amplitudes are:

$$\begin{aligned} \left\{ \begin{array}{l} \mathcal{T}_{WW}^{(2a)} \\ \mathcal{T}_{WW}^{(2b)} \end{array} \right\} &= \left( -\frac{g}{\sqrt{2}} \right)^4 (B_{ei}^*)^2 (B_{\mu j})^2 \lambda_j \lambda_i^* M_j M_i (-1) \\ &\times \int \frac{d^4 q}{(2\pi)^4} \frac{1}{(q^2 - M_i^2)(q^2 - M_j^2)(q^2 - M_W^2)^2} \left\{ \begin{array}{l} [\bar{u}(k') \gamma_\mu \gamma_\nu P_R u_c(k)] [\bar{u}_c(p') \gamma^\mu \gamma^\nu P_L u(p)] \\ [\bar{u}(k') \gamma_\mu \gamma_\nu P_R u_c(k)] [\bar{u}_c(p') \gamma^\nu \gamma^\mu P_L u(p)] \end{array} \right\}. \end{aligned} \quad (\text{B12})$$

We denoted as  $u_c$  the  $u$ -spinors associated to the positively charged fermions (usually considered ‘‘antiparticles’’), but operationally these are normal  $u$ -spinors. The factor  $(-1)$  before the integral is important and comes from the Wick contractions of the fermion fields with the external states, given the sign convention of the previous diagrams. Using the identities

$$\gamma^\mu \gamma^\nu = g^{\mu\nu} - i\sigma^{\mu\nu}, \quad \sigma_{\mu\nu} \gamma^5 = \frac{i}{2} \epsilon_{\mu\nu\alpha\beta} \sigma^{\alpha\beta}, \quad (\text{B13})$$

the spinor structure in both amplitudes of Eq. (B12) can be simplified to the same form:

$$[\gamma_\mu \gamma_\nu P_R] [\gamma^\mu \gamma^\nu P_L] = [\gamma_\mu \gamma_\nu P_R] [\gamma^\nu \gamma^\mu P_L] = 4 [P_R] [P_L]. \quad (\text{B14})$$

This is the reason why the diagrams in Fig. 2 do not cancel but, on the contrary, they add to twice their value.

Using the following Fierz identity:

$$2 [\bar{u}_1 P_R u_2] [\bar{u}_3 P_L u_4] = [\bar{u}_1 \gamma_\alpha P_L u_4] [\bar{u}_3 \gamma^\alpha P_R u_2] \quad (\text{B15})$$

we can transform the spinor product into a product of currents. The amplitudes of Eq. (B12) then result in:

$$\mathcal{T}_{WW}^{(2a)} = \mathcal{T}_{WW}^{(2b)} = -i \frac{\alpha_w^2}{2M_W^2} (B_{ei}^*)^2 (B_{\mu j})^2 \lambda_j \lambda_i^* \sqrt{x_i x_j} \mathcal{J}(x_i, x_j) [\bar{u}(k') \gamma_\alpha P_L u(p)] [\bar{u}_c(p') \gamma^\alpha P_R u_c(k)] . \quad (\text{B16})$$

Now, the diagrams with Goldstone bosons instead of  $W$ 's contain scalar currents which, in analogy to Eqs. (B11), should be transformed before doing the Wick contractions according to:

$$\bar{\psi}_\mu(x) P_{L,R} n_j(x) = \lambda_j \bar{n}_j(x) P_{L,R} \psi_\mu^c(x), \quad (\text{B17a})$$

$$\bar{n}_i(x) P_{L,R} \psi_e(x) = \lambda_i^* \bar{\psi}_e^c(x) P_{L,R} n_i(x). \quad (\text{B17b})$$

Besides this detail, the calculation of the diagrams of Fig. 2 with one or two Goldstone bosons replacing the  $W$ 's follows the same steps as above.

From Eq. (B16) and the analogous expressions corresponding to the diagrams with Goldstone bosons, it is clear that both diagrams of Fig. 2 give identical results.

We should now transform the  $u$ -spinors of the positively charged fermions into  $v$ -spinors, as it is customary, using the following conjugated current identity:

$$\bar{u}_c(p') \gamma^\alpha P_R u_c(k) = \bar{v}(k) \gamma^\alpha P_L v(p') \quad (\text{B18})$$

and use the Fierz identity (B8) to arrive at the same spinor structure as in the amplitude of Fig. 1, namely Eq. (B10). The total result for Fig. 2 is then:

$$\begin{aligned} \mathcal{T}^{(2)} &\equiv \sum_{\kappa=a,b} \left[ \mathcal{T}_{WW}^{(\kappa)} + \mathcal{T}_{GG}^{(\kappa)} + \mathcal{T}_{GW+WG}^{(\kappa)} \right] \\ &= i \frac{\alpha_w^2}{4M_W^2} (B_{ei}^*)^2 (B_{\mu j})^2 \lambda_j \lambda_i^* G_{\text{Box}}(x_i, x_j) [\bar{u}(k') \gamma_\alpha P_L u(p)] [\bar{v}(k) \gamma^\alpha P_L v(p')] , \end{aligned} \quad (\text{B19})$$

where the function  $G_{\text{Box}}$  is given in Eq. (12), which is identical to that of Ref. [12].

The sum of all diagrams is  $\mathcal{T}^{(1)} + \mathcal{T}^{(2)}$  [ Eqs. (B10) and (B19)]; from this amplitude one deduces the effective coupling  $G_{M\bar{M}}$  of Eq. (10).

- [1] B. Pontecorvo, Sov. Phys. JETP **6**, 429 (1957).
- [2] G. Feinberg and S. Weinberg, Phys. Rev. **123**, 1439 (1961).
- [3] B.W. Lee and R.E. Shrock, Phys. Rev. **D16**, 1444 (1977); A. Halprin, Phys. Rev. Lett. **48**, 1313 (1982); A. Halprin and A. Masiero, Phys. Rev. **D48**, R2987 (1993); P. Herczeg and R.N. Mohapatra, Phys. Rev. **D46**, 5200 (1992); A. Ilakovac, Phys. Rev. **D62**, 036010 (2000); for a review of the physics, see also Y. Kuno and Y. Okada, Rev. Mod. Phys. **73**, 151 (2001).
- [4] T. Huber *et al.*, Phys. Rev. **D41**, 2709 (1990); B. Matthias *et al.*, Phys. Rev. Lett. **66**, 2716 (1991); R. Abela *et al.*, Phys. Rev. Lett. **77**, 1950 (1996); L. Willmann *et al.*, Phys. Rev. Lett. **82**, 49 (1999).
- [5] For a review on muonium physics see L. Willmann and K. Jungmann, Physics **499**, 43 (1997); and more recently, K. Jungmann, Proc. of Memorial Symp. in Honor of V. W. Hughes, New Haven, Connecticut, 14-15 Nov 2003, e-print nucl-ex/0404013, Apr 2004. 20pp.
- [6] G. Cvetič, C. Dib, C. S. Kim and J. D. Kim, Phys. Rev. D **66**, 034008 (2002) [arXiv:hep-ph/0202212].
- [7] A. Ilakovac, Phys. Rev. **D62**, 036010 (2000).
- [8] T. E. Clark and S. T. Love, Mod. Phys. Lett. A **19**, 297 (2004) [arXiv:hep-ph/0307264].
- [9] We use the standard relativistic norm for the states  $\{a_p, a_p^\dagger\} = 2E_p(2\pi)^3 \delta^3(p - p')$  and for the spinors  $u(p)^\dagger u(p) = 2E_p$ .
- [10] Our mass mixing  $m_{M\bar{M}}$  corresponds to  $2\delta$  of Ref. [2].
- [11] E. Nardi, E. Roulet and D. Tommasini, Phys. Lett. B **327**, 319 (1994); *ibid.* **344**, 225 (1995).
- [12] A. Ilakovac and A. Pilaftsis, Nucl. Phys. B **437**, 491 (1995) [arXiv:hep-ph/9403398].
- [13] C. Itzykson and J.-B. Zuber, *Quantum Field Theory* (McGraw-Hill, New York, 1980).
- [14] B. Kayser, F. Gibrat-Debu, and F. Perrier, *The Physics of Massive Neutrinos* (World Scientific, Singapore, 1989).
- [15] J. A. Aguilar-Saavedra, Int. J. Mod. Phys. C **8**, 147 (1997) [arXiv:hep-ph/9607313].
- [16] B. Kayser, Phys. Rev. D **30**, 1023 (1984).

- [17] A. Pilaftsis, *Z. Phys. C* **55**, 275 (1992) [arXiv:hep-ph/9901206].
- [18] E. Witten, *Nucl. Phys. B* **268**, 79 (1986); R. N. Mohapatra and J. W. Valle, *Phys. Rev. D* **34**, 1642 (1986); J. L. Hewett and T. G. Rizzo, *Phys. Rept.* **183** (1989) 193.
- [19] D. Wyler and L. Wolfenstein, *Nucl. Phys. B* **218**, 205 (1983).
- [20] G. C. Branco, M. N. Rebelo and J. W. F. Valle, *Phys. Lett. B* **225**, 385 (1989).
- [21] M. C. Gonzalez-Garcia and J. W. Valle, *Phys. Lett. B* **216**, 360 (1989).
- [22] S. Eidelman *et al.* [Particle Data Group], *Phys. Lett. B* **592**, 1 (2004).
- [23] J. N. Bahcall, P. I. Krastev and A. Yu. Smirnov, *Phys. Rev. D* **58**, 096016 (1998) [arXiv:hep-ph/9807216]; M. C. Gonzalez-García *et al.*, *Nucl. Phys. B* **573**, 3 (2000) [arXiv:hep-ph/9906469]; G. L. Fogli *et al.*, *Phys. Rev. D* **62**, 013002 (2000) [arXiv:hep-ph/9912231]; A. S. Joshipura and M. Nowakowski, *Phys. Rev. D* **51**, 2421 (1995) [arXiv:hep-ph/9408224].